AJNR

Brain Abnormalities in Becker Muscular Dystrophy: Evaluation by Voxel-Based DTI and Morphometric Analysis

Hiroyuki Maki, Madoka Mori-Yoshimura, Hiroshi Matsuda, Yasumasa Hashimoto, Miho Ota, Yukio Kimura, Yoko Shigemoto, Naoko Ishihara, Hirohito Kan, Emiko Chiba, Elly Arizono, Sumiko Yoshida, Yuji Takahashi and Noriko Sato

Brain Abnormalities in Becker Muscular Dystrophy: Evaluation by Voxel-Based DTI and Morphometric Analysis

Hiroyuki Maki, Madoka Mori-Yoshimura, Hiroshi Matsuda, Yasumasa Hashimoto, Miho Ota, Yukio Kimura, Yoko Shigemoto, Naoko Ishihara, Hirohito Kan, Emiko Chiba, Elly Arizono, Sumiko Yoshida, Yuji Takahashi, and Noriko Sato

ABSTRACT

BACKGROUND AND PURPOSE: Although various neuropsychological problems in Becker muscular dystrophy have attracted attention, there have been few related neuroimaging studies. We investigated brain abnormalities in patients with Becker muscular dystrophy using 3D T1WI and DTI.

MATERIALS AND METHODS: MR images were obtained for 30 male patients and 30 age-matched healthy male controls. We classified patients into Dp140+ and Dp140− subgroups based on their predicted dystrophin Dp140 isoform expression and performed voxel-based comparisons of gray and white matter volumes and DTI metrics among the patients, patient subgroups, and controls. ROI-based DTI analyses were also performed.

RESULTS: Significantly decreased fractional anisotropy was observed in the left planum temporale and right superior parietal lobule compared between the Becker muscular dystrophy and control groups. In the Dp140− subgroup, decreased fractional anisotropy was observed in the left planum temporale, but no significant changes were seen in the Dp140+ subgroup. The ROI-based analysis obtained the same results. No significant differences were evident in the gray or white matter volumes or the DTI metrics other than fractional anisotropy between the groups.

CONCLUSIONS: A DTI metric analysis is useful to detect white-matter microstructural abnormalities in Becker muscular dystrophy that may be affected by the Dp140 isoform expression.

ABBREVIATIONS: AD = axial diffusivity; BMD = Becker muscular dystrophy; DARTEL = Diffeomorphic Anatomical Registration Through Exponentiated Lie Algebra; DMD = Duchenne muscular dystrophy; FA = fractional anisotropy; IQ = intelligence quotient; MD = mean diffusivity; RD = radial diffusivity; VBM = voxel-based morphometry; WAIS = Wechsler Adult Intelligence Scale

Becker muscular dystrophy (BMD) is an X-linked recessive form of muscular dystrophy caused by mutations in the

dystrophin gene that lead to the production of variable levels of partially functioning dystrophin.[1] Compared with the more severe allelic disorder Duchenne muscular dystrophy (DMD), individuals with BMD have a much longer normal life expectancy.[2] In addition to muscle weakness, mutations in the dystrophin gene have been linked to cognitive impairment. For example, learning and behavioral problems are well-revealed in individuals with DMD.[3] Although it has not been established whether similar neuropsychological problems are part of the BMD disease spectrum, several studies have described attention problems, language/speech delays, and mental problems such as depression and neurosis in individuals with BMD.[4-6]

The dystrophin gene is the largest gene, containing 79 exons and tightly regulated tissue-specific promoters that make a range of protein isoforms known to reflect their relative sizes. These include the longest dystrophin isoform, Dp427, and the shorter products: Dp71, Dp116, Dp140, and Dp260.[7] A genotype-phenotype relationship between mutations in the dystrophin gene and cognitive function has been described.[8] Intellectual impairment is

more prominent in patients with DMD with mutations in the distal part of the dystrophin gene (distal to exon 44) that are associated with the loss of expression of the Dp140 isoform.[8] The role of Dp140 in BMD has been reported to be important.[9]

Functional and quantitative neuroimaging studies of DMD have revealed multiple abnormalities, including gray matter volume differences, altered white matter microstructural integrity as measured using DTI, and metabolic derangement shown by PET.[10,11] DTI analyses have demonstrated widespread and significant white matter abnormalities in individuals with DMD lacking Dp140 expression compared with those with retained Dp140 expression and healthy controls.[10,12] However, the existing neuroimaging studies of BMD are limited to a visual-assessment study on brain atrophy and a DTI study using ROI methodology.[6,13] No quantitative evaluation of whole-brain morphology and microstructures in BMD has been reported.

Voxel-based morphometry (VBM) and DTI are commonly used methods in studies of neurodegenerative and psychiatric diseases. VBM visualizes morphologic brain differences, and DTI estimates microstructural parameters such as fractional anisotropy (FA), mean diffusivity (MD), axial diffusivity (AD), and radial diffusivity (RD), mainly in the white matter.[14,15] In the present study, we conducted both VBM and DTI analyses to clarify the morphologic and microstructural features in patients with BMD and the group-level differences in BMD subtypes based on Dp140 expression.

MATERIALS AND METHODS

This retrospective study was approved by the Ethics Committee of Japan's National Center of Neurology and Psychiatry Hospital (Tokyo). The requirement for patients' informed consent was waived due to the retrospective nature of the study. We enrolled 39 male patients with BMD who visited our hospital and underwent MR imaging between January 2014 and December 2021. The diagnosis of BMD was based on typical symptoms (eg, delayed motor milestones, proximal weakness, hypertrophied calves, and elevated creatine kinase levels) and deletions of the dystrophin gene or reduced dystrophin levels confirmed by a muscle biopsy.[1] All the patients' diagnoses of BMD were reviewed and confirmed by an experienced neurologist.

Seven patients were excluded from this study because of a lack of 3D T1WI or DTI data. We also excluded 2 patients with multiple lacunar infarcts on MR imaging. A final total of 30 men with BMD was included in the study. We also recruited 30 age-matched healthy male controls on the basis of the following criteria: no history of neurologic or psychiatric diseases, no contact with psychiatric services, and no use of medication that affects the central nervous system. Written informed consent was obtained from each healthy control participant.

We retrospectively collected information regarding the disease duration of patients with BMD, ambulatory performance, and steroid treatment from their medical records. Information regarding intelligence test scores on the Wechsler Adult Intelligence Scale III (WAIS-III) was also collected. The WAIS-III was used to measure verbal intelligence quotient (IQ), performance IQ, and full-scale IQ.

Genetic Diagnoses

Information regarding the patients' genetic diagnoses was collected from their medical records. We classified the patients with BMD into 2 subgroups according to mutations that might alter Dp140 expression. Duplication, deletion, or small mutations in the genic region between the Dp140 promoter and the N-terminal and frameshift or nonsense mutations involving intron 44 or downstream were deemed to be Dp140 expression modifiers. Among these possible modifiers, we considered harmful Dp140 mutations (Dp140−) as deletion mutations, which included the Dp140 start codon and/or coding region or coding region nonsense or splice site variants.[6]

MR Imaging Acquisition

In all participants, MR imaging was performed using a 3T clinical scanner (Achieva; Philips Healthcare) with a 32-channel head coil. 3D sagittal T1-weighted images were acquired (TR/TE, 7.18/3.46; flip angle, 10°; effective section thickness, 0.6 mm; slab thickness, 180 mm; matrix, 384 × 384; FOV, 261 × 261 mm; number of excitations, 1), yielding 300 contiguous slices through the brain. Single-shot spin-echo echo-planar DWIs were obtained with the following parameters: TR/TE, 6700/58 ms; flip angle, 90°; effective section thickness, 3.0 mm with no gap; slices, 60; matrix, 80 × 78; FOV, 240 × 240 mm; number of excitations, 2; noncoplanar diffusion directions, 15; b-values, 0 and 1000 s/mm^2. This study used a cross-sectional design, and the MR imaging for each subject was performed only once.

VBM Analysis

To investigate morphologic differences in gray and white matter volumes, we segmented and spatially normalized the 3D T1-weighted images using the Statistical Parametric Mapping 12 software program (SPM12; http://www.fil.ion.ucl.ac.uk/spm/) running in Matlab (MathWorks) with the Diffeomorphic Anatomical Registration through Exponentiated Lie Algebra (DARTEL; part of SPM) technique.[16] The segmented gray and white matter images were normalized to the Montreal Neurological Institute space using the DARTEL technique and smoothed with an 8-mm full width at half maximum Gaussian kernel.

ROI-Based Analysis of Gray and White Matter Volumes

The potential disparities of gray and white matter volumes between the patients with BMD and controls were also investigated using the FreeSurfer program (Version 6.0; http://surfer.nmr.mgh.harvard.edu/). The 3D T1-weighted images were processed using the recon-all processing stream (https://surfer.nmr.mgh.harvard.edu/fswiki/recon-all), and the gray and white matter volumes were parcellated into 34 bilateral ROIs as defined by the Desikan-Killiany atlas.[17] The total intracranial volumes were also measured.

Postprocessing and Analysis of the DTI Data

We performed a voxel-based whole-brain comparison for DTI analyses that has been validated.[18] First, we added the denoising step and Gibbs-ringing correction using MRtrix3 (https://www.mrtrix.org/).[19,20] After eddy current correction and brain

extraction using FSL, Version 5.0 (https://fsl.fmrib.ox.ac.uk/fsl/fslwiki), we fitted the diffusion tensor model in each voxel derived from the data with a b-value of 1000 using the DTIFit function (https://fsl.fmrib.ox.ac.uk/fsl/fslwiki/FDT/UserGuide) to estimate the FA, MD, AD, and RD maps.[15,21]

For the investigation of DTI metrics on a voxel-by-voxel basis, we spatially normalized these images using the DARTEL registration method. Each 3D T1-weighted image was coregistered and resliced to its $b=0$ image. Subsequently, the coregistered 3D T1-weighted images were spatially normalized using the DARTEL template. Finally, the transformation matrix was applied to DTI metric maps. Each image was then smoothed using an 8-mm full width at half maximum Gaussian kernel. To restrict the analysis to regions of white matter, we masked the DTI metrics maps with the binary mask image made by the segmented white matter images derived from each individual 3D T1-weighted image that was coregistered and resliced to its $b=0$ image.

ROI-Based DTI Analysis

In addition to the voxel-based analyses, we performed an ROI-based analysis. The ROI of each significant cluster in the voxel-based analysis derived from SPM12 was automatically mapped to normalized DTI metrics images using MRIcron software (https://people.cas.sc.edu/rorden/mricron/). We investigated the left-right asymmetry of the measured DTI metrics values by reflecting the ROI of each significant cluster to the corresponding hemisphere — if it included the planum temporale or planum polare — because these areas are reported to be highly asymmetric.[22] Each ROI was flipped to the other hemisphere using MRIcro software (https://people.cas.sc.edu/rorden/mricro/). The flipped ROIs were then evaluated with the MRIcron software. To assess the asymmetry of the DTI metrics values, we evaluated the ratio of left and right ROIs between the patients with BMD and controls.

Statistical Analyses

Demographic data are presented as mean (SD), range, or percentage, as indicated. The Mann-Whitney U test was used to analyze continuous data, and the Fisher exact test was used to analyze binary data. All statistical analyses were performed using Bell-Curve (Social Survey Research Information) for Excel software (Microsoft), and a 2-tailed P value $< .05$ was regarded as significant.

To determine the differences among the patients with BMD, the BMD subgroups classified by the expression of the Dp140 isoform, and the control group, we subjected the normalized gray and white matter volumes and DTI values to a 2-sample t test analysis using SPM12. The significance of the differences in gray and white matter volumes was tested with patient age and the total intracranial volume (calculated by SPM12) as confounding covariates. The DTI values were statistically analyzed using patient age as a confounding variable. For all SPM analyses, the significance level was set at a family-wise error–corrected $P < .05$ at voxel-level and a cluster size of >100 voxels. A normalized template provided by SPM12 (single_subj_T1.nii) was used for visualization. We used Bell-Curve for Excel software to perform a 2-sample t test to examine the difference of each ROI and the

ratio of left and right ROIs between the patients with BMD and the controls. A 2-tailed P value $< .05$ was regarded as significant. We performed an ANCOVA to evaluate differences in the volume of each ROI between the BMD and control groups, controlling for patient age and total intracranial volume. The significance level of the statistical analysis was set at Bonferroni corrected $P < .05$.

RESULTS

Clinical Characteristics

The clinical characteristics of each subject group are summarized in the Online Supplemental Data. The mean ages of the patients with BMD and controls were 37.8 (SD, 12.5) and 38.9 (SD, 12.2) years, respectively. No significant differences in age were observed among the groups (BMD versus controls, $P = .78$; BMD_Dp140− versus controls, $P = .81$; BMD_Dp140+ versus controls, $P = .45$; and BMD_Dp140− versus BMD_Dp140+, $P = .41$). Among the 30 patients with BMD, the genetic diagnoses identified deletion mutations ($n = 20$, 66.7%), duplication mutations ($n = 2$, 6.7%), small mutations ($n = 6$, 20.0%), and others (diagnosed by immunohistochemistry; $n = 2$, 6.7%). Eighteen patients had deleterious Dp140 mutations (BMD_Dp140−), and 10 patients did not have deleterious Dp140 mutations (BMD_Dp140+). Among the 30 patients with BMD, 21 (70%) patients were ambulant and 9 (30%) were wheelchair-bound; the mean age at loss of ambulation was 32.2 (SD, 9.3) years. Four patients were on steroid treatment, with a mean treatment duration of 3.6 years (range, 2–9 years). No significant differences were noted in the duration of steroid treatment between the Dp140 expression subgroups ($P = .68$).

The WAIS-III data were available for 16 patients, and the scores are listed in the Online Supplemental Data. The full-scale IQ of the patients was within the normal range (≥ 70). No significant differences were observed in the WAIS-III scores between the BMD_Dp140+ and BMD_Dp140− subgroups.

Voxel-Based Morphometric and DTI Analyses

The results of the VBM analysis revealed no significant differences in either gray or white matter between the groups, ie, BMD versus controls; BMD_Dp140− versus controls; BMD_Dp140+ versus controls; and BMD_Dp140− versus patients with BMD_Dp140+. In the voxel-based DTI analysis, the 30 patients with BMD showed areas with significantly decreased FA in the left planum temporale and right superior parietal lobule compared with the healthy controls (Table 1 and Fig 1). Eighteen patients with BMD_Dp140− presented with significant FA reductions in the left planum temporale compared with controls (Table 1 and Fig 2). In contrast, the 10 patients with BMD_Dp140+ presented with no significant differences in FA compared with the BMD_Dp140− group and controls (data not shown). MD, AD, and RD values showed no significant differences in all group comparisons (data not shown).

ROI-Based Analysis of Gray and White Matter Volumes

No significant difference was observed in the gray or white matter volumes between the patients with BMD and the controls ($P > .05$).
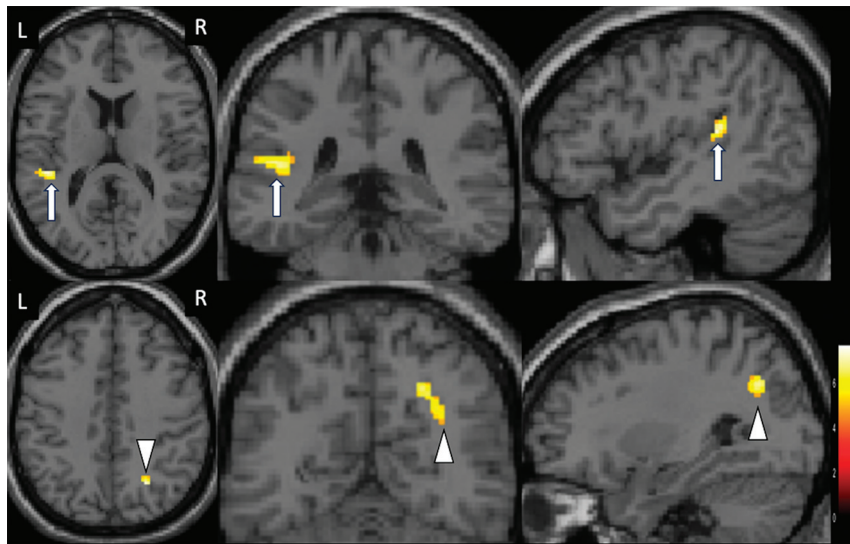
Table 1: Results of the voxel-based FA analysis of white matter between the 30 patients with BMD and 30 controls and between the patients with BMD_Dp140− (n = 18) and healthy controls (n = 30)ᵃ

				MNI Coordinates			
Analysis	df	Cluster Size	T Value	x	y	z	Regions of Peaks
Controls > BMD	57	222	7.67	−45	−34	15	Left planum temporale
		204	7.34	24	−62	42	Right superior parietal lobule
Controls > BMD_Dp140−	45	151	6.63	−46	−34	15	Left planum temporale

Note:—MNI indicates Montreal Neurological Institute.
ᵃ All clusters are significant at a voxel level of P < .05 (family-wise error–corrected) and a cluster size of >100 voxels.

FIG 1. Results of the voxel-based FA analysis between the patients with BMD (n = 30) and controls (n = 30) (P < .05, family-wise error–corrected, voxel level). The FA was significantly decreased in the left planum temporale (*arrows*) and right superior parietal lobule (*arrowheads*) of the patients with BMD. The background images are single_subj_T1 images, which are regarded as one of the anatomically standardized images in the SPM12 toolbox. The color scale represents *t* values. L indicates left; R, right.
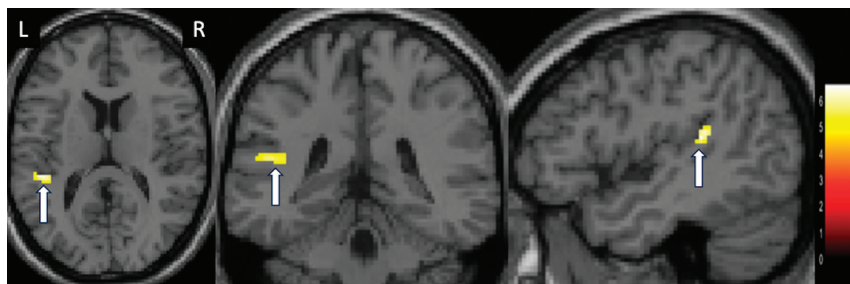
FIG 2. Results of the voxel-based FA analysis between the patients with BMD_Dp140− (n = 18) and controls (n = 30) (P < .05, family-wise error–corrected, voxel-level). The FA was significantly decreased in the left planum temporale (*arrows*) of the patients with BMD_Dp140−. The color scale represents *t* values. L indicates left; R, right.

ROI-Based DTI Analysis

As shown in Table 2, there was a significant difference in FA values in both the left planum temporale and the right superior parietal lobule between the BMD and control groups (P < .01 respectively). Between the 18 patients with BMD_Dp140− and the 30 controls, significant differences in FA values were observed in the left planum temporale (P < .01) (Table 3). The ratio of the left-right ROIs of FA values in the planum temporale showed significant differences between the BMD and control group and between the 18

patients with BMD_Dp140− and the control group (P < .01 respectively) (Tables 2 and 3).

DISCUSSION

We investigated VBM and DTI metrics in patients with BMD and observed significant FA reductions in the patients' left planum temporale and right superior parietal lobule compared with the healthy controls. The subgroup analyses revealed that the patients with BMD_Dp140− (but not the patients with BMD_Dp140+) had reduced FA in the left planum temporale. To our knowledge, this is the first published investigation of the microstructural differences between individuals with BMD and healthy controls using VBM and DTI analyses. Our findings suggest that the Dp140 dystrophin isoform may play an important role in microstructural abnormalities of the left planum temporale in individuals with BMD.

Neuroimaging studies in large cohorts of patients with DMD have revealed FA reductions in both the supratentorial and infratentorial white matter and indicated that Dp140 expression contributed to the FA changes in patients with DMD.[10,12] Our present findings demonstrate impaired white matter integrity in the BMD group, and the range of abnormality is more limited than that of patients with DMD. This finding may indicate that BMD manifests with less severity compared with DMD.[7] Our comparison of BMD subtypes with the healthy controls revealed significant FA abnormalities in the Dp140− group but not in the Dp140+ group. The differences between the BMD_Dp140− subgroup and controls indicated that the expression of the Dp140 isoform could affect microstructural abnormalities in individuals with BMD and those with DMD. No significant difference was detected in Dp140 expression based on IQ scores; this may be because the intelligence test scores of some of the patients with more severe conditions may not have been available.

Table 2: Comparison of FA values of the ROIs located in the left planum temporale and those flipped to the right hemisphere between the 30 patients with BMD and 30 controls, and the ratio of FA values for the left and right ROIs[a]

	Controls (*n* = 30)			BMD (*n* = 30)			
	Mean	SD	Range	Mean	SD	Range	*P* Value
Left planum temporale	0.29	0.04	0.21–0.40	0.23	0.04	0.16–0.30	<.01
ROIs flipped to the right	0.32	0.05	0.23–0.42	0.29	0.05	0.22–0.41	
Ratio of left-right ROIs	0.9	0.13	0.68–1.14	0.8	0.16	0.47–1.09	<.01
Right superior parietal lobule	0.34	0.03	0.28–0.42	0.29	0.04	0.25–0.34	<.01

[a] A comparison of FA values of the ROIs located in the right superior parietal lobule is also shown.

Table 3: The FA values of the ROIs located in the left planum temporale and the ROIs flipped to the other hemisphere in 18 patients with BMD_Dp140− and 30 controls

	Controls (*n* = 30)			BMD_Dp140− (*n* = 18)			
	Mean	SD	Range	Mean	SD	Range	*P* Value
Left planum temporale	0.3	0.04	0.22–0.41	0.23	0.03	0.17–0.27	*P* < .01
ROIs flipped to the right	0.33	0.05	0.24–0.43	0.31	0.02	0.23–0.36	
Ratio of left-right ROIs	0.91	0.13	0.69–1.2	0.78	0.17	0.49–1.09	*P* < .01

Earlier DTI investigations of patients with DMD reported a significant increase in MD values in the white matter compared with controls.[10,12] Contrary to this result, we observed no significant differences in MD between the present BMD and control groups. MD is a measure that can be affected by the barriers that restrict the movement of water, such as cell membranes.[23] The loss of the shorter isoforms of dystrophin was reported to be associated with reduced levels of aquaporin-4, a protein involved in membrane permeability.[24,25] The difference in MD between individuals with DMD and those with BMD may be related to the differential cumulative loss of brain-expressed isoforms, affected by the mutation site along the gene. Axonal degeneration was described as sensitive to AD, whereas demyelination was deemed to be sensitive to RD.[26] We observed no significant differences in AD or RD between the present patients with BMD and controls, similar to our findings regarding MD. This result suggests that individuals with BMD may exhibit less-severe axonal and myelin abnormalities.

The present patients with BMD showed reduced FA in the left planum temporale. The established functional lateralization of the left cerebral hemisphere for language functions in most individuals has been confirmed, and the planum temporale has been presumed to be involved in auditory processing.[22] Patients with BMD have been reported to have poor verbal working memory despite intact long-term memory and acquired knowledge.[5] Verbal working memory is thought to reflect a distributed brain network consisting of the frontal lobe and hippocampus.[27] Functional MR imaging and electroencephalography studies have indicated an important role of the primary auditory area in the active maintenance of verbal memory and the support of verbal working memory.[28,29] We thus speculate that the temporal areas with decreased FA in our present patients with BMD may have caused their poor verbal working memory.

In contrast to the alterations in FA, no significant differences in gray or white matter volumes were noted between the BMD and control groups in this study. An investigation of patients with DMD by a VBM analysis showed local gray matter reductions compared with healthy controls.[10] Both the muscles and brains of individuals with DMD have been reported to be completely missing the full-length 427 kDa dystrophin protein (Dp427), which is normally located in the cerebral cortex.[30] Dp427 may be present in small amounts or partially functioning in the brains and muscles of patients with BMD, thus resulting in the absence of significant differences in brain volumes between the present BMD and control groups.

There are some study limitations to consider. A voxel-based analysis is useful for identifying very subtle anatomic changes but is sensitive to registration accuracy. To reduce the effect of misregistration on the statistical analysis, we applied smoothing to the normalized images. We used the conventionally used default smoothing kernel (8-mm Gaussian filter). However, smoothing might aggravate the partial volume problem.[15] Our study was further limited by the small sample size of subgroups of patients with BMD, and the study should, therefore, be viewed as a preliminary study and requires confirmation in larger samples. Because this was a retrospective study, the cognitive profiles of some of the participants were not evaluated by neuropsychological tests. Prospective studies that include more detailed neuropsychological examinations are necessary to investigate the correlation between brain abnormalities and cognitive impairment in patients with BMD.

CONCLUSIONS

We conducted VBM and DTI analyses in patients with BMD, and we observed significantly reduced FA in the left planum temporale in all patients with BMD and in the BMD_Dp140− subgroup compared with the healthy controls, but not in the BMD_Dp140+ subgroup. These results indicate that the Dp140 dystrophin isoform may contribute to temporal microstructural abnormalities in BMD.

ACKNOWLEDGMENTS

10.1038/s41439-022–00217–6), for supporting the psychological assessment and data handling.

REFERENCES

1. Bushby KM, Gardner-Medwin D. **The clinical, genetic and dystrophin characteristics of Becker muscular dystrophy, I: natural history.** *J Neurol* 1993;240:98–104 CrossRef Medline
2. Monaco AP, Bertelson CJ, Liechti-Gallati S, et al. **An explanation for the phenotypic differences between patients bearing partial deletions of the DMD locus.** *Genomics* 1988;2:90–95 CrossRef Medline
3. Hinton VJ, De Vivo DC, Nereo NE, et al. **Poor verbal working memory across intellectual level in boys with Duchenne dystrophy.** *Neurology* 2000;54:2127–32 CrossRef Medline
4. Koeks Z, Hellebrekers DM, van de Velde NM, et al. **The neurocognitive profile of adults with Becker muscular dystrophy in the Netherlands.** *J Neuromuscul Dis* 2022;9:543–53 CrossRef Medline
5. Young HK, Barton BA, Waisbren S, et al. **Cognitive and psychological profile of males with Becker muscular dystrophy.** *J Child Neurol* 2008;23:155–62 CrossRef Medline
6. Mori-Yoshimura M, Mizuno Y, Yoshida S, et al. **Psychiatric and neurodevelopmental aspects of Becker muscular dystrophy.** *Neuromuscul Disord* 2019;29:930–39 CrossRef Medline
7. Muntoni F, Torelli S, Ferlini A. **Dystrophin and mutations: one gene, several proteins, multiple phenotypes.** *Lancet Neurol* 2003;2:731–40 CrossRef Medline
8. Felisari G, Martinelli Boneschi F, Bardoni A, et al. **Loss of dp140 dystrophin isoform and intellectual impairment in Duchenne dystrophy.** *Neurology* 2000;55:559–64 CrossRef Medline
9. Chamova T, Guergueltcheva V, Raycheva M, et al. **Association between loss of dp140 and cognitive impairment in Duchenne and Becker dystrophies.** *Balkan J Med Genet* 2013;16:21–30 CrossRef Medline
10. Doorenweerd N, Straathof CS, Dumas EM, et al. **Reduced cerebral gray matter and altered white matter in boys with Duchenne muscular dystrophy.** *Ann Neurol* 2014;76:403–11 CrossRef Medline
11. Lee JS, Pfund Z, Juhász C, et al. **Altered regional brain glucose metabolism in Duchenne muscular dystrophy: a PET study.** *Muscle Nerve* 2002;26:506–12 CrossRef Medline
12. Preethish-Kumar V, Shah A, Kumar M, et al. **In vivo evaluation of white matter abnormalities in children with Duchenne muscular dystrophy using DTI.** *AJNR Am J Neuroradiol* 2020;41:1271–78 CrossRef Medline
13. Biagi L, Lenzi S, Cipriano E, et al. **Neural substrates of neuropsychological profiles in dystrophinopathies: a pilot study of diffusion tractography imaging.** *PLoS One* 2021;16:e0250420 CrossRef Medline
14. Ashburner J, Friston KJ. **Voxel-based morphometry: the methods.** *Neuroimage* 2000;11:805–21 CrossRef Medline
15. Abe O, Takao H, Gonoi W, et al. **Voxel-based analysis of the diffusion tensor.** *Neuroradiology* 2010;52:699–710 CrossRef Medline
16. Ashburner J. **A fast diffeomorphic image registration algorithm.** *Neuroimage* 2007;38:95–113 CrossRef Medline
17. Seiger R, Ganger S, Kranz GS, et al. **Cortical thickness estimations of FreeSurfer and the CAT12 toolbox in patients with Alzheimer's disease and healthy controls.** *J Neuroimaging* 2018;28:515–23 CrossRef Medline
18. Ota M, Sato N, Maikusa N, et al. **Whole brain analyses of age-related microstructural changes quantified using different diffusional magnetic resonance imaging methods.** *Jpn J Radiol* 2017;35:584–89 CrossRef Medline
19. Kellner E, Dhital B, Kiselev VG, et al. **Gibbs-ringing artifact removal based on local subvoxel-shifts.** *Magn Reson Med* 2016;76:1574–81 CrossRef Medline
20. Veraart J, Novikov DS, Christiaens D, et al. **Denoising of diffusion MRI using random matrix theory.** *Neuroimage* 2016;142:394–406 CrossRef Medline
21. Smith SM. **Fast robust automated brain extraction.** *Hum Brain Mapp* 2002;17:143–55 CrossRef Medline
22. Dorsaint-Pierre R, Penhune VB, Watkins KE, et al. **Asymmetries of the planum temporale and Heschl's gyrus: relationship to language lateralization.** *Brain* 2006;129:1164–76 CrossRef Medline
23. Clark KA, Nuechterlein KH, Asarnow RF, et al. **Mean diffusivity and fractional anisotropy as indicators of disease and genetic liability to schizophrenia.** *J Psychiatr Res* 2011;45:980–88 CrossRef Medline
24. Frigeri A, Nicchia GP, Nico B, et al. **Aquaporin-4 deficiency in skeletal muscle and brain of dystrophic mdx mice.** *FASEB j* 2001;15:90–98 CrossRef Medline
25. Ricotti V, Roberts RG, Muntoni F. **Dystrophin and the brain.** *Dev Med Child Neurol* 2011;53:12 CrossRef Medline
26. Shizukuishi T, Abe O, Aoki S. **Diffusion tensor imaging analysis for psychiatric disorders.** *Magn Reson Med Sci* 2013;12:153–59 CrossRef Medline
27. Bidelman GM, Brown JA, Bashivan P. **Auditory cortex supports verbal working memory capacity.** *Neuroreport* 2021;32:163–68 CrossRef Medline
28. Emch M, von Bastian CC, Koch K. **Neural correlates of verbal working memory: an FMRI meta-analysis.** *Front Hum Neurosci* 2019;13:180 CrossRef Medline
29. Ferrero A, Rossi M. **Cognitive profile and neuropsychiatric disorders in Becker muscular dystrophy: a systematic review of literature.** *Neurosci Biobehav Rev* 2022;137:104648 CrossRef Medline
30. Kim TW, Wu K, Black IB. **Deficiency of brain synaptic dystrophin in human Duchenne muscular dystrophy.** *Ann Neurol* 1995;38:446–49 CrossRef Medline